STUDIES OF IN-MEDIUM MODIFICATION OF DIJETS IN PbPb COLLISIONS AT 5.02 TeV WITH THE CMS DETECTOR*

Jussi Viinikainen

for the CMS Collaboration

Vanderbilt University, USA

Received 10 August 2022, accepted 29 August 2022, published online 14 December 2022

Jet quenching is a well-established signature of quark–gluon plasma formation in heavy-ion collisions. Studies of the transverse momentum balance of back-to-back jets, as well as medium-induced modifications to jet shapes and fragmentation functions, provide important experimental constraints on quark–gluon plasma properties. Using a large sample of dijet events from 5.02 TeV lead–lead and proton–proton collisions recorded by the CMS, we study quenching effects differentially with respect to the dijet transverse momentum balance. We use short-range correlations between jets and charged particles to assess medium-induced modifications to jet substructures on each side of the dijet. The path-length-dependent energy loss and energy density fluctuations are also probed using long-range correlations between jets and charged particles.

DOI:10.5506/APhysPolBSupp.16.1-A59

1. Introduction

Jet–hadron correlation method is well suited for studying parton energy loss within quark–gluon plasma. It has been previously applied for example in studies of charged hadron momentum as a function of radial distance from the jet axis [1, 2]. The results presented in these proceedings build upon these previous analyses and take advantage of the large PbPb dataset at $\sqrt{s_{NN}} = 5.02$ TeV with integrated luminosity of 1.69 nb^{-1} recorded in 2018 by the CMS detector [3] together with a *pp* dataset with integrated luminosity of 320 pb^{-1} recorded in 2017. We measure the charged particle momentum profiles in a dijet system around both leading and subleading jet axes as

* Presented at the 29$^{\text{th}}$ International Conference on Ultrarelativistic Nucleus–Nucleus Collisions: Quark Matter 2022, Kraków, Poland, 4–10 April, 2022.

a function of the dijet momentum balance $x_j = \frac{p_{\mathrm{T}}^{\mathrm{sub}}}{p_{\mathrm{T}}^{\mathrm{lead}}}$ [4]. Categorizing the distributions with x_j provides a handle in studying path-length-dependent energy loss and energy loss fluctuations.

Jet–hadron correlations is a flexible method, and can also be used to study the azimuthal anisotropies of the jets via the Fourier expansion coefficients v_n. When the initial collision region of the heavy ions has an almond-like shape, the jets are expected to lose less energy in the in-plane direction compared to the out-of-plane direction [5]. This results in a measurable jet v_2 signal. The higher order v_n coefficients reflect medium density or initial state geometry fluctuations. The results presented in these proceedings introduce a new method for the jet anisotropy measurements [6]. The azimuthal anisotropies in these proceedings are measured exclusively for a dijet system, which is why we denote the corresponding Fourier coefficients as v_n^{dijet}.

2. Jet–hadron correlations

Correlations between jets and charged particles are studied using two-dimensional distributions of the relative pseudorapidity $\Delta\eta$ and relative azimuth $\Delta\varphi$ of the charged particles with respect to the jet axis. These distributions are constructed by pairing each charged particle with the leading jet and the subleading jet, separately, and are normalized by the number of dijets.

Since the detector has a limited acceptance in η, it is more likely to find jet–hadron pairs with small rather than large $\Delta\eta$ values. Thus, the raw correlation shapes have the charged-particle yield falling rapidly towards large $\Delta\eta$. A mixed event procedure, where jets are paired with charged particles from different events, is employed to correct for these acceptance effects and possible detector inefficiencies. Denoting the number of dijets satisfying the selection criteria as N_{dijet}, the per-dijet associated charged-particle yield, corrected for acceptance effects, is given by

$$\frac{1}{N_{\mathrm{dijet}}} \frac{\mathrm{d}^2 N}{\mathrm{d}\Delta\eta \, \mathrm{d}\Delta\varphi} = \frac{\mathrm{ME}(0,0)}{\mathrm{ME}(\Delta\eta, \Delta\varphi)} S(\Delta\eta, \Delta\varphi) \,, \tag{1}$$

where N is the number of jet–hadron pairs, the signal pair distribution $S(\Delta\eta, \Delta\varphi)$ represents the per-dijet normalized yield of jet–hadron pairs from the same event, and $\mathrm{ME}(\Delta\eta, \Delta\varphi)$ is the mixed-event pair distribution. The ratio $\mathrm{ME}(0,0)/\mathrm{ME}(\Delta\eta, \Delta\varphi)$ is the normalized correction factor. The maximum of the mixed-event distribution can be found at $(0,0)$ since no pairs with $\Delta\eta = 0$ are lost as a consequence of acceptance effects.

After performing the acceptance correction, we need to separate the long-range correlations from the jet-like correlations. Since jet correlations are short-range correlations, we can use jet–hadron pairs with large pseudorapidity gap $1.5 < |\Delta\eta| < 2.5$ in the near side of the distribution ($\Delta\varphi < \pi/2$) to estimate the contribution from the long-range correlations. Since leading and subleading jets are statistically back-to-back and come from the same events, we can get the long-range correlations in the whole $\Delta\varphi$ range by combining the contributions that are estimated from the near sides of leading and subleading jet–hadron distributions and shifting the subleading one by π. Subtracting this long-range-correlation distribution from the acceptance corrected one gives the short-range-correlated distribution.

3. Short-range correlations

From the short-range correlations, we determine the charged particle radial momentum profiles around the jet axis, also known as jet shapes, using the equation

$$\rho(\Delta r) = \frac{1}{\delta r}\frac{1}{N_{\text{jets}}}\frac{\Sigma_{\text{jets}}\Sigma_{\text{tracks}\in(\Delta r_a,\,\Delta r_b)}p_{\text{T}}^{\text{ch}}}{\Sigma_{\text{jets}}\Sigma_{\text{tracks}\in\Delta r<1}\,p_{\text{T}}^{\text{ch}}}\,, \tag{2}$$

where Δr_a and Δr_b define the annular edges of Δr, and $\delta r = \Delta r_b - \Delta r_a$. This is done differentially as a function of charged particle transverse momentum p_{T}^{ch}, centrality, and dijet momentum balance x_j.

The results for leading jets are presented in Fig. 1 and for subleading jets in Fig. 2. Concentrating on the x_j dependence of the results, which is the new result in this analysis, we can see that leading and subleading jets have different trends. The leading jets show the greatest modifications with respect to *pp* reference in balanced events, while the subleading jets are the most modified in unbalanced events. The results are consistent with a hypothesis that the unbalanced events are more surface biased, leading to the subleading jet going through a much larger distance in the plasma compared to the leading jet. However, one needs to take into account energy loss fluctuations before any conclusions can be drawn.

Outside of the jet cone radius $R = 0.4$, the PbPb-to-*pp* ratio for subleading jets in unbalanced events gets closer to one. This is due to a change in the *pp* reference. One can see from the left-hand side plot in Fig. 2 that there is an enhancement of high p_{T}^{ch} particles around $\Delta r = 0.5$ for the unbalanced *pp* case. This is due to the fact that to create an unbalanced configuration in *pp* case, there is likely to be a third jet in the subleading side to balance out the momentum.

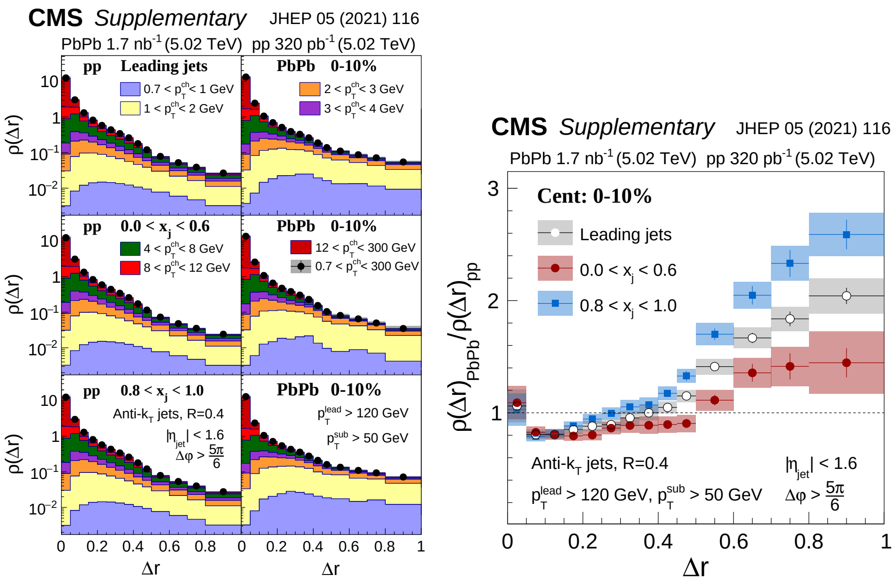

Fig. 1. Left: Jet shape distributions from leading jet–hadron correlations in *pp* and 0–10% central PbPb collisions presented in different x_j selections [4]. Right: Ratios of PbPb-to-*pp* jet shapes for different x_j selections [4].

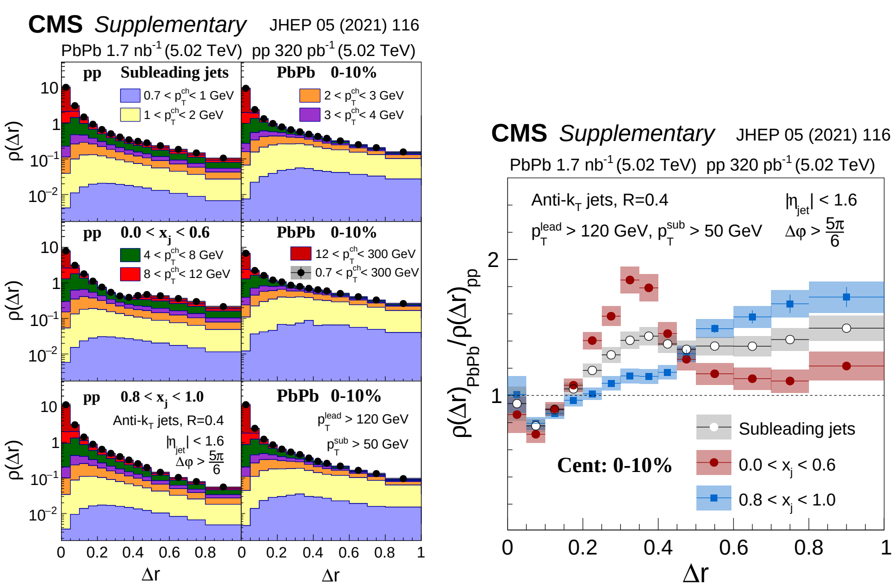

Fig. 2. Left: Jet shape distributions from subleading jet–hadron correlations in *pp* and 0–10% central PbPb collisions presented in different x_j selections [4]. Right: Ratios of PbPb-to-*pp* jet shapes for different x_j selections [4].

4. Long-range correlations

The long-range-correlation distribution is fitted with a Fourier fit up to the fourth order

$$f_{\text{Fourier}}(\Delta\varphi) = A\left(1 + \sum_{n=1}^{4} 2V_{n\Delta}\cos(n\Delta\varphi)\right), \tag{3}$$

where A is an overall normalization factor and $V_{n\Delta}$ is the Fourier coefficient of the order of n. Since we are fitting a jet–hadron distribution, the obtained $V_{n\Delta}$ components are a mixture of dijet and hadron v_n. Assuming no remaining nonflow contributions, $V_{n\Delta}^{\text{jet}-\text{hadron}}$ factorizes [7, 8] as

$$V_{n\Delta}^{\text{jet}-\text{hadron}} = v_n^{\text{dijet}}\, v_n^{\text{hadron}}, \tag{4}$$

from which v_n^{dijet} is solved for. The v_n^{hadron} coefficient is factorized from dihadron correlations requiring the same p_{T}^{ch} bin for the trigger and associated hadrons. The away-side jet peak is explicitly removed from the jet–hadron-correlation distribution as described in Section 2. Since there is no jet information for dihadrons, we need to restrict the analysis to $p_{\text{T}}^{\text{ch}} < 3$ GeV to keep the impact of the away-side jet contribution to v_n^{hadron} small.

The v_n^{dijet} results as a function of centrality factorized from the hadron p_{T} region of $0.7 < p_{\text{T}}^{\text{ch}} < 3$ GeV are presented in Fig. 3. For v_2^{dijet}, we see a rising trend towards more peripheral events up to 30–50% centrality bin. As the collision region becomes more almond-like for these more peripheral collisions, the in-plane *versus* the out-of-plane path-length difference gets more pronounced, causing this trend. Both v_3^{dijet} and v_4^{dijet} are compatible to zero, meaning that we do not observe a measurable impact from medium density or initial-state geometry fluctuations.

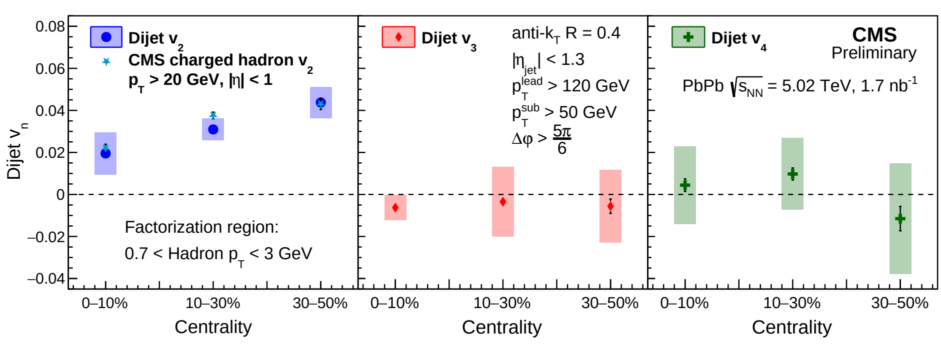

Fig. 3. Dijet v_n as a function of centrality factorized from the region $0.7 < p_{\text{T}}^{\text{ch}} < 3$ GeV [6].

We also provide a comparison between the average of the multiparticle cumulant v_2 results at $p_{\mathrm{T}} > 20$ GeV and $|\eta| < 1$ from Ref. [9] and v_2^{dijet} in Fig. 3. High-p_{T} particles are likely to originate from jets, and even though the jet population and kinematic regions are different, the underlying physics is the same and thus it is interesting to make a qualitative comparison to the v_2^{dijet} results. Indeed, we see that the high-p_{T} hadron results agree with v_2^{dijet} within the uncertainties of the measurements.

5. Summary

The CMS Collaboration has used the jet–hadron correlation method to study the path-length-dependent parton energy loss in dijet events. We observe the greatest widening of the jet shapes for leading jets in lead–lead collisions with respect to proton–proton collisions in events where the dijet momentum is balanced. For subleading jets, the modifications are the greatest in events with significant dijet momentum imbalance. Both of these observations are consistent with a hypothesis that unbalanced dijet events are more surface-biased compared to the balanced dijet events. We have further measured the Fourier expansion coefficients v_n for dijets, and observe positive and centrality-dependent v_2^{dijet}. This can be interpreted as a result of the in-plane *versus* the out-of-plane path-length difference getting larger for more peripheral events, leading to a larger difference in energy loss between these two directions. The higher-order coefficients are consistent with zero.

REFERENCES

[1] CMS Collaboration, *J. High Energy Phys.* **1611**, 055 (2016), `arXiv:1609.02466 [nucl-ex]`.

[2] CMS Collaboration, *J. High Energy Phys.* **1805**, 006 (2018), `arXiv:1803.00042 [nucl-ex]`.

[3] CMS Collaboration, *J. Instrum.* **3**, S08004 (2008).

[4] CMS Collaboration, `arXiv:2101.04720 [hep-ex]`.

[5] X.-N. Wang, *Phys. Rev. C* **63**, 054902 (2001), `arXiv:nucl-th/0009019`.

[6] CMS Collaboration, CMS Physics Analysis Summary, CMS-PAS-HIN-21-002, 2022.

[7] M. Luzum, *Phys. Lett. B* **696**, 499 (2011), `arXiv:1011.5773 [nucl-th]`.

[8] CMS Collaboration, *Eur. Phys. J. C* **72**, 2012 (2012), `arXiv:1201.3158 [nucl-ex]`.

[9] CMS Collaboration, *Phys. Lett. B* **776**, 195 (2018), `arXiv:1702.00630 [hep-ex]`.